

Passivity-based Output Synchronization in $SE(3)$

Yuji Igarashi, Takeshi Hatanaka, Masayuki Fujita and Mark W. Spong

Abstract—In this paper, we address an output synchronization problem in the Special Euclidean group of dimension three ($SE(3)$) under the situation that rigid-bodies modeled in $SE(3)$ exchange information along strongly connected graphs. We develop a velocity control law, which is defined only by local information i.e. information of neighbors on position errors and relative orientations. The achievement of the output synchronization and hence the convergence of all the rigid-bodies to any prescribed trajectory is proven by using a property called passivity. Our results are also extended to the case with delays in communication among rigid-bodies. Finally, we demonstrate the effectiveness of the present input through numerical simulations and experiments.

I. INTRODUCTION

Cooperative control is an active area of current research [1], [2] in systems and control community with numerous practical applications such as sensor networks, robot networks, coordinate control of satellites and formation control of aircrafts. The goal in cooperative control problems is to design a distributed control strategy such that the aggregate system attains specified tasks, such as consensus, flocking, coordination or formation control [3], [4], [5], [6].

Among the papers concerning cooperative control, the most recent and closely related works to this paper are the passivity-based control of multi-agent systems [7], [8], [9]. In [7] and [8], output synchronization problems are studied, where the achievement of output synchronization is proven by using the sum of storage functions as the Lyapunov function candidate. As shown in these references, passivity-based control enables one to handle communication delays and switching topology within a unified (energy-based) framework.

In most of the previous works, the agents are assumed to be point masses. However, in many real systems such as underwater vehicles, satellites and visual feedback systems, it is more natural to model the configuration of each agent as an element of the Special Euclidean group of dimension three $SE(3) := \mathcal{R}^3 \times SO(3)$.

In this paper, we address the output synchronization problem in $SE(3)$ based on some techniques developed in [7], [8] and [10]. We consider a network of n rigid-bodies in $SE(3)$ whose interconnection is represented by a strongly connected communication graph. The goal of this paper is to develop a velocity coordination law that will result in the convergence of the outputs of the rigid-bodies to any common desirable

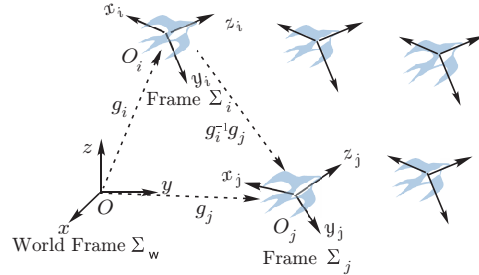


Fig. 1. Rigid Body Motion in $SE(3)$

trajectory. The present velocity coordination law is based on a passivity-like property and the positive definite function presented in [11], and only requires relative positions and orientations of neighbors defined by the graph. We show that output synchronization is achieved under some assumptions using the proposed velocity input. Then, our results are also extended to the case with time delays in communication. The novel features of this paper are as follows.

- We consider output synchronization in $SE(3)$. There exist a few works [12] considering such a problem, where control laws are presented so that the synchronization, balancing and circular formations in $SE(3)$ of identical particles are achieved. However, their control law requires information other than relative orientations in limited communication. In contrast, this paper presents a velocity input completely defined by the relative information even in the limited communication.
- This paper achieves both position and attitude coordination, whereas [10], [13] investigated only the attitude coordination in almost the same problem setting.
- The present input can make all the rigid-bodies converge to any time-varying trajectories such as Kuramoto oscillator unlike most of the previous works on output synchronization where the convergence to a constant value is investigated.
- The assumption on the graph of the strong connectivity is milder than the other works on the energy function based approaches [7], [8], [10], where the graph is assumed to be balanced.

This paper is organized as follows. Section II formulates rigid-body motion in $SE(3)$ and a graph structure under consideration in this paper. In Section III, we first show that the rigid-body motion in $SE(3)$ has a passivity-like property, and introduce an output synchronization problem. Then, a velocity input is proposed based on the passivity-like property and achievement of output synchronization is proven. We also show if there exist communication delays, output synchronization is still attained. We demonstrate our results through numerical simulations and experiments in Section IV. Conclusions are finally drawn in Section V.

Yuji Igarashi, Takeshi Hatanaka and Masayuki Fujita are with the Department of Mechanical and Control Engineering, Tokyo Institute of Technology, Tokyo 152-8552, JAPAN fujita@ctrl.titech.ac.jp

M.W. Spong is with the Coordinated Science Laboratory and Department of Electrical and Computer Engineering, University of Illinois at Urbana-Champaign, Urbana, IL 61801 USA mspong@uiuc.edu

This work was in part supported by Japan Society for the Promotion of Science Grant-in-Aid for Scientific Research (C) No. 19560437

II. SYSTEM DESCRIPTION

Throughout this paper, we consider the motion of a group of n rigid bodies in 3-dimensional space (see Figure 1). Let Σ_w be an inertial coordinate frame and $\Sigma_i, i \in \{1, \dots, n\}$ a body-fixed coordinate frame whose origin is located at the center of mass of body i . Assume that all the coordinate frames are right-handed and Cartesian. We denote by $p_i \in \mathcal{R}^3$ the position of the rigid body $i \in \{1, \dots, n\}$ in a fixed inertial coordinate frame Σ_w . We will use $e^{\hat{\xi}_i \theta_i} \in \mathcal{R}^{3 \times 3}$ to represent the rotation matrix of a body-fixed frame Σ_i relative to an inertial coordinate frame Σ_w . Here, $\xi_i \in \mathcal{R}^3$, $\xi_i^T \xi_i = 1$ and $\theta_i \in \mathcal{R}$ specify the direction of rotation and the angle of rotation, respectively. The notation ‘ \wedge ’ (wedge) is the skew-symmetric operator from \mathcal{R}^3 to the space of 3×3 skew-symmetric matrices, namely

$$\begin{bmatrix} \xi_1 \\ \xi_2 \\ \xi_3 \end{bmatrix}^\wedge = \begin{bmatrix} 0 & -\xi_3 & \xi_2 \\ \xi_3 & 0 & -\xi_1 \\ -\xi_2 & \xi_1 & 0 \end{bmatrix}.$$

The notation ‘ \vee ’ (vee) denotes the inverse operator to ‘ \wedge ’. The transformation $e^{\hat{\xi}_i \theta_i}$ is orthogonal with unit determinant i.e. an element of the Special Orthogonal group $SO(3)$. A configuration consists of the pair $(p_i, e^{\hat{\xi}_i \theta_i})$ and hence the configuration space of the rigid-body motion is the Special Euclidean group $SE(3)$, which is the product space of \mathcal{R}^3 with $SO(3)$. We use the 4×4 matrix

$$g_i = \begin{bmatrix} e^{\hat{\xi}_i \theta_i} & p_i \\ 0 & 1 \end{bmatrix}, \quad i \in \{1, \dots, n\}$$

as the homogeneous representation of $(p_i, e^{\hat{\xi}_i \theta_i}) \in SE(3)$.

Let us now introduce the velocity of each rigid body to represent the rigid-body motion of the frame Σ_i relative to Σ_w . Define the body velocity $V_i^b := (v_i, \omega_i)$ and

$$\hat{V}_i^b = \begin{bmatrix} \hat{\omega}_i & v_i \\ 0 & 0 \end{bmatrix}, \quad i \in \{1, \dots, n\},$$

where $v_i \in \mathcal{R}^3$ and $\omega_i \in \mathcal{R}^3$ are the linear and angular velocities of body i relative to Σ_i respectively. Then, each rigid-body motion is represented by the kinematic model

$$\dot{g}_i = g_i \hat{V}_i^b, \quad i \in \{1, \dots, n\}. \quad (1)$$

The main advantages to using the above homogeneous representation are global and geometric descriptions of rigid-body motion. For more details on the rigid-body motion in $SE(3)$, refer to [14], [15].

The interconnection of a network of rigid bodies is represented by a weighted and directed graph $G = (\mathcal{V}, \mathcal{E}, \mathcal{W})$ where $\mathcal{V} := \{1, \dots, n\}$, $\mathcal{E} \subset \mathcal{V} \times \mathcal{V}$ and \mathcal{W} are the node set, the edge set and the positive weight set, respectively. The neighbors of body i are defined as [2] $\mathcal{N}_i := \{j \in \mathcal{V} \mid (j, i) \in \mathcal{E}\}$. Namely, agent i received information from agent j if $j \in \mathcal{N}_i$. The weights $w_{ij} > 0$ represent the reliability of each communication link. We moreover define the weighted graph Laplacian matrix

$$L_w := [L_{wij}] = \begin{cases} \sum_{j \in \mathcal{N}_i} w_{ij} & \text{if } j = i, \\ -w_{ij} & \text{if } j \in \mathcal{N}_i, \\ 0 & \text{if } j \notin \mathcal{N}_i, \end{cases}$$

which plays an important role in this paper.

In this paper, we make the following assumptions.

- A1: The information graph among the rigid-bodies is fixed and strongly connected.
- A2: There exists no delay in the information graph.

Though we temporarily assume A2 in the next section, the problem without this assumption will be examined in Section III-D.

III. OUTPUT SYNCHRONIZATION IN $SE(3)$

This section presents a velocity input, and proves that the input achieves the output synchronization.

A. Passivity-like Property in $SE(3)$

We first show that the kinematic model (1) possess a passivity-like property and we use this property to develop a output feedback law for output synchronization. For this purpose, we first define the total energy of translation and rotation

$$\begin{aligned} \psi(g_i) &:= \|J(I_4 - g_i)\|_F^2, & J &:= \begin{bmatrix} \frac{1}{\sqrt{2}} I_3 & 0 \\ 0 & 1 \end{bmatrix} \\ &= \frac{1}{2} \|p_i\|^2 + \phi(e^{\hat{\xi}_i \theta_i}), & \phi(e^{\hat{\xi}_i \theta_i}) &:= \frac{1}{2} \text{tr}(I_3 - e^{\hat{\xi}_i \theta_i}) \end{aligned}$$

where I_n is the $n \times n$ identity matrix, $\|\cdot\|_F$ represents the Frobenius matrix norm ($\|A\|_F = \text{tr}(A^T A)^{1/2}$) and $\|\cdot\|$ the Euclidean vector norm. By the definition, $\psi(g_i) = 0$ if and only if $g_i = I_4$.

Lemma 1: The time derivative of $\psi(g_i)$ along the trajectories of (1) satisfies

$$\dot{\psi}(g_i) = (V_i^b)^T \Pi_i, \quad V_i^b = \begin{bmatrix} v_i \\ \omega_i \end{bmatrix}, \quad \Pi_i := \begin{bmatrix} e^{-\hat{\xi}_i \theta_i} p_i \\ \mathbf{sk}(e^{\hat{\xi}_i \theta_i})^\vee \end{bmatrix},$$

where $\mathbf{sk}(e^{\hat{\xi}_i \theta_i})$ is a skew-symmetric part of the matrix $e^{\hat{\xi}_i \theta_i}$, i.e. $\mathbf{sk}(e^{\hat{\xi}_i \theta_i}) := \frac{1}{2}(e^{\hat{\xi}_i \theta_i} - e^{-\hat{\xi}_i \theta_i})$.

Proof: Immediate from ([11] pp. 42, Lemma 1). ■

If we now consider the velocity V_i^b as an input and the vector form of the rigid-body motion Π_i as an output, Lemma 1 says that the rigid-body motion in $SE(3)$ (1) is passive from the input V_i^b to the output Π_i (This property is called a *passivity-like* property throughout this paper) in the sense defined in [16], since integrating (2) from 0 to T yields

$$\int_0^T (V_i^b)^T \Pi_i dt = \psi(g_i(T)) - \psi(g_i(0)) \geq -\psi(g_i(0)).$$

B. Output Synchronization in $SE(3)$

Next we define output synchronization as follows.

Definition 1 (Output Synchronization): A group of n rigid bodies is said to achieve output synchronization, if

$$\lim_{t \rightarrow \infty} \psi(g_i^{-1} g_j) = 0 \quad \forall i, j \in \{1, \dots, n\}. \quad (2)$$

By the definition of the function ψ , equation (2) implies the outputs of all the rigid bodies converge to a common value. From the definition of the output, it means that both of positions and orientations converge to a common value (Figure 2).

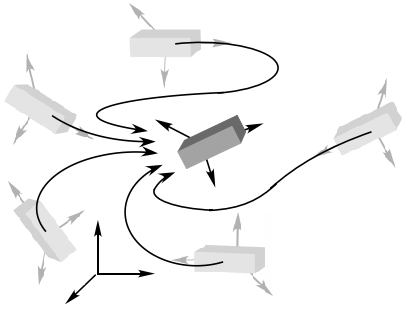


Fig. 2. Output Synchronization in SE(3)

C. Design of Velocity Input

In this paper, we present the velocity input

$$V_i^b = \begin{bmatrix} e^{-\hat{\xi}_i \theta_i} & 0 \\ 0 & e^{-\hat{\xi}_i \theta_i} \end{bmatrix} \begin{bmatrix} v_d \\ e^{-\hat{\xi}_d \theta_d} \omega_d \end{bmatrix} + K_i \sum_{j \in \mathcal{N}_i} w_{ij} \begin{bmatrix} e^{-\hat{\xi}_i \theta_i} & 0 \\ 0 & I \end{bmatrix} \begin{bmatrix} p_j - p_i \\ \mathbf{sk}(e^{-\hat{\xi}_i \theta_i} e^{\hat{\xi}_j \theta_j})^\vee \end{bmatrix}, \quad (3)$$

where $K_i = \begin{bmatrix} k_{pi} I & 0 \\ 0 & k_{ei} I \end{bmatrix}$, $k_{pi} > 0$ and $k_{ei} > 0$ are gains for the position error and attitude error respectively. In addition, ω_d is defined by $\omega_d := e^{-\hat{\xi}_d \theta_d} \dot{e}^{\hat{\xi}_d \theta_d}$. v_d and ω_d are desired linear and angular velocity.

The present input (3) consists of two parts (feedforward and feedback laws). The first term is the feedforward part, which specifies a desirable behavior after the output synchronization is achieved. Thus, the functions v_d and ω_d should be common among all the rigid-bodies. After the output synchronizes, the velocity input becomes

$$V_i^b = \begin{bmatrix} e^{-\hat{\xi}_i \theta_i} & 0 \\ 0 & e^{-\hat{\xi}_i \theta_i} \end{bmatrix} \begin{bmatrix} v_d \\ e^{-\hat{\xi}_d \theta_d} \omega_d \end{bmatrix}. \quad (4)$$

Thus all rigid bodies have the same linear and angular velocity because output synchronization implies $e^{\hat{\xi}_i \theta_i} = e^{\hat{\xi}_j \theta_j}$. Furthermore all of rigid bodies can track the common desired trajectory by designing the v_d and ω_d appropriately.

Although there are a few exceptions in [17], the convergence to a constant value has been investigated in most of the previous works on cooperative control. For example, in [2], the convergence value is determined by the average or weighted average of agent's initial states. In the leader following cases of [3] and [18], the convergence value is a constant state of the leader. In contrast, the present input achieves the convergence to any desired velocity. Note that the problem and approach in this paper are also quite different from [17], where a consensus algorithm is presented so that each vehicle reaches consensus on a time varying reference state.

The second term is the feedback part, which assures the output synchronization. This term is also divided into the position and rotation error feedback parts. Our proposed velocity control scheme is easy to implement, since it depends only on local information received from neighbors. This means that each agent needs only the relative position and orientation between its own reference frame and that of its neighbors.

We next show that the velocity input (3) achieves output synchronization. This is proven based on the fact that strongly connected graphs have the following properties [19].

Lemma 2: *If the graph is strongly connected, there exists a vector γ satisfying*

$$\gamma^T L_w = 0 \quad \gamma^T = [\gamma_1, \dots, \gamma_n], \quad \gamma_i > 0 \quad \forall i, \quad (5)$$

where n is the number of vertices of the graph.

Theorem 1: *Suppose that there exist n rigid-bodies represented by (1). Then, under the assumptions A1 and A2, the velocity input (3) achieves the output synchronization if $\bar{e}^{\hat{\xi}_i \theta_i} := e^{-\hat{\xi}_d \theta_d} e^{\hat{\xi}_i \theta_i} \quad \forall i$ are positive definite.*

Proof: Define a potential function by

$$U := \sum_{i=1}^n \gamma_i \left(\frac{1}{2k_{pi}} \|\bar{p}_i\|^2 + \frac{1}{k_{ei}} \phi(\bar{e}^{\hat{\xi}_i \theta_i}) \right), \quad (6)$$

where $\bar{p}_i := p_i - \int_0^t v_d dt$ and γ_i are vectors satisfying

$$\gamma^T L_w = 0 \quad \gamma^T = [\gamma_1, \dots, \gamma_n], \quad \gamma_i > 0 \quad \forall i. \quad (7)$$

It follows from the assumption A1 and Lemma 2 that there exists a vector satisfying (7). This potential function U is defined as a weighted sum of the energy functions $\psi(g_i)$ and used as a Lyapunov function candidate. This choice is quite natural from the viewpoint that the kinematic model (1) possesses the passivity-like property.

Differentiating (6) yields

$$\begin{aligned} \dot{U} &= \sum_{i=1}^n \gamma_i \left[\mathbf{sk}(\bar{e}^{\hat{\xi}_i \theta_i})^\vee \right]^T \begin{bmatrix} \frac{1}{k_{pi}} I & 0 \\ 0 & \frac{1}{k_{ei}} I \end{bmatrix} \\ &\quad \left(\begin{bmatrix} e^{\hat{\xi}_i \theta_i} & 0 \\ 0 & I \end{bmatrix} V_i^b - \begin{bmatrix} v_d \\ e^{-\hat{\xi}_i \theta_i} e^{\hat{\xi}_d \theta_d} \omega_d \end{bmatrix} \right) \\ &= \sum_{i=1}^n \sum_{j \in \mathcal{N}_i} \gamma_i w_{ij} \left[\mathbf{sk}(\bar{e}^{\hat{\xi}_i \theta_i})^\vee \right]^T \begin{bmatrix} p_j - p_i \\ \mathbf{sk}(e^{-\hat{\xi}_i \theta_i} e^{\hat{\xi}_j \theta_j})^\vee \end{bmatrix} \\ &= \sum_{i=1}^n \sum_{j \in \mathcal{N}_i} \gamma_i w_{ij} \left[\mathbf{sk}(\bar{e}^{\hat{\xi}_i \theta_i})^\vee \right]^T \\ &\quad \begin{bmatrix} p_j - \int_0^t v_d dt - (p_i - \int_0^t v_d dt) \\ \mathbf{sk}(e^{-\hat{\xi}_i \theta_i} e^{\hat{\xi}_d \theta_d} e^{-\hat{\xi}_d \theta_d} e^{\hat{\xi}_j \theta_j})^\vee \end{bmatrix} \\ &= \sum_{i=1}^n \sum_{j \in \mathcal{N}_i} \gamma_i w_{ij} \left[\mathbf{sk}(\bar{e}^{\hat{\xi}_i \theta_i})^\vee \right]^T \begin{bmatrix} \bar{p}_j - \bar{p}_i \\ \mathbf{sk}(\bar{e}^{-\hat{\xi}_i \theta_i} \bar{e}^{\hat{\xi}_j \theta_j})^\vee \end{bmatrix} \\ &= \sum_{i=1}^n \sum_{j \in \mathcal{N}_i} \gamma_i w_{ij} \{ \bar{p}_i^T (\bar{p}_j - \bar{p}_i) \\ &\quad + (\mathbf{sk}(\bar{e}^{\hat{\xi}_i \theta_i})^\vee)^T \mathbf{sk}(\bar{e}^{-\hat{\xi}_i \theta_i} \bar{e}^{\hat{\xi}_j \theta_j})^\vee \}. \quad (8) \end{aligned}$$

By using a completing square, the term of $\bar{p}_i^T (\bar{p}_j - \bar{p}_i)$ is rewritten as

$$\bar{p}_i^T (\bar{p}_j - \bar{p}_i) = -\frac{1}{2} \|\bar{p}_i\|^2 + \frac{1}{2} \|\bar{p}_j\|^2 - \frac{1}{2} \|(\bar{p}_i - \bar{p}_j)\|^2. \quad (9)$$

We next obtain

$$\begin{aligned} & \left(\mathbf{sk}(\bar{e}^{\hat{\xi}_i \theta_i})^\vee \right)^T \mathbf{sk}(\bar{e}^{-\hat{\xi}_i \theta_i} \bar{e}^{\hat{\xi}_j \theta_j})^\vee \\ &= -\phi(\bar{e}^{\hat{\xi}_i \theta_i}) + \phi(\bar{e}^{\hat{\xi}_j \theta_j}) \\ &\quad - \frac{1}{4} \text{tr} \left((\bar{e}^{\hat{\xi}_i \theta_i} + \bar{e}^{-\hat{\xi}_i \theta_i}) (I - \bar{e}^{-\hat{\xi}_i \theta_i} \bar{e}^{\hat{\xi}_j \theta_j}) \right) \quad (10) \end{aligned}$$

from the fact that $a^T b = -\frac{1}{2} \text{tr}(\hat{a}\hat{b})$ holds for any 3-dimensional vector $a \in \mathcal{R}^3, b \in \mathcal{R}^3$ [10, Theorem 1]. Since $\lambda_{\min}(B)\text{tr}(A) \leq \text{tr}(AB)$ holds true for any positive semi-definite symmetric matrices $A \in \mathcal{R}^{n \times n}, B \in \mathcal{R}^{n \times n}$ [21], we have

$$\begin{aligned} & -\text{tr} \left((\bar{e}^{\hat{\xi}_i \theta_i} + \bar{e}^{-\hat{\xi}_i \theta_i})(I - \bar{e}^{-\hat{\xi}_j \theta_j} e^{\hat{\xi}_i \theta_i}) \right) \\ & \leq -\lambda_{\min}(\bar{e}^{\hat{\xi}_i \theta_i} + \bar{e}^{-\hat{\xi}_i \theta_i}) \text{tr}(I - \bar{e}^{-\hat{\xi}_j \theta_j} \bar{e}^{\hat{\xi}_i \theta_i}), \end{aligned} \quad (11)$$

where $\lambda_{\min}(B)$ denotes the minimal eigenvalue of B . Notice $-\lambda_{\min}(\bar{e}^{\hat{\xi}_i \theta_i} + \bar{e}^{-\hat{\xi}_i \theta_i}) > 0$ from the assumption of $\bar{e}^{\hat{\xi}_i \theta_i} > 0 \forall i$. Thus, the deviation of the potential function (6) satisfies the inequality

$$\begin{aligned} \dot{U} & \leq \sum_{i=1}^n \sum_{j \in \mathcal{N}_i} \gamma_i w_{ij} \left(-\bar{U}_i + \bar{U}_j - \frac{1}{2} \|(\bar{p}_i - \bar{p}_j)\|^2 \right. \\ & \quad \left. - \frac{1}{2} \lambda_{\min}(\bar{e}^{\hat{\xi}_i \theta_i} + \bar{e}^{-\hat{\xi}_i \theta_i}) \phi(\bar{e}^{-\hat{\xi}_i \theta_i} \bar{e}^{\hat{\xi}_j \theta_j}) \right), \end{aligned} \quad (12)$$

where $\bar{U}_i := \frac{1}{2} \|\bar{p}_i\|^2 + \phi(\bar{e}^{\hat{\xi}_i \theta_i})$. Now, the term $\sum_{i=1}^n \sum_{j \in \mathcal{N}_i} \gamma_i w_{ij} (-\bar{U}_i + \bar{U}_j)$ is equivalent to

$$\sum_{i=1}^n \sum_{j \in \mathcal{N}_i} \gamma_i w_{ij} (-\bar{U}_i + \bar{U}_j) = -\gamma^T L_w \begin{bmatrix} \bar{U}_1 \\ \vdots \\ \bar{U}_n \end{bmatrix} = 0. \quad (13)$$

This yields the following inequality, and hence the deviation of the potential function is nonpositive definite.

$$\begin{aligned} \dot{U} & \leq -\frac{1}{2} \sum_{i=1}^n \sum_{j \in \mathcal{N}_i} \gamma_i w_{ij} (\|\bar{p}_i - \bar{p}_j\|^2 \\ & \quad + \lambda_{\min}(\bar{e}^{\hat{\xi}_i \theta_i} + \bar{e}^{-\hat{\xi}_i \theta_i}) \phi(\bar{e}^{-\hat{\xi}_i \theta_i} \bar{e}^{\hat{\xi}_j \theta_j})) \\ & \leq 0 \end{aligned} \quad (14)$$

We finally prove the convergence of the output by using the LaSalle's invariant principle [20]. Before proving it, we define the set

$$E := \{g_i \in SE(3), \forall i \mid \bar{e}^{\hat{\xi}_i \theta_i} > 0 \dot{U} \equiv 0\}. \quad (15)$$

From the assumption of $\bar{e}^{\hat{\xi}_i \theta_i} > 0$ and (14), we have

$$\dot{U} = 0 \Rightarrow \|\bar{p}_i - \bar{p}_j\|^2 = 0, \phi(\bar{e}^{-\hat{\xi}_i \theta_i} \bar{e}^{\hat{\xi}_j \theta_j}) = 0, (j, i) \in \mathcal{E} \quad (16)$$

Because of the strong connectivity of the graph, the set E is replaced by

$$\begin{aligned} E & = \{g_i \in SE(3), \forall i \mid \bar{e}^{\hat{\xi}_i \theta_i} > 0 \\ & \quad \|\bar{p}_i - \bar{p}_j\|^2 = 0 \phi(\bar{e}^{-\hat{\xi}_i \theta_i} \bar{e}^{\hat{\xi}_j \theta_j}) = 0 \forall i, j\} \\ & = \{g_i \in SE(3), \forall i \mid \bar{e}^{\hat{\xi}_i \theta_i} > 0 \\ & \quad \|p_i - p_j\|^2 = 0 \phi(e^{-\hat{\xi}_i \theta_i} e^{\hat{\xi}_j \theta_j}) = 0 \forall i, j\} \\ & = \{g_i \in SE(3), \forall i \mid \bar{e}^{\hat{\xi}_i \theta_i} > 0 \psi(g_i^{-1} g_j) = 0 \forall i, j\}. \end{aligned} \quad (17)$$

In addition, the inputs (3) of all the rigid-bodies are equal in the case of $g_i = g_j \forall i, j$. This implies that the set E is an invariant set. Consequently, we have (2) and the output synchronization is achieved. ■

Remark 1: The positive definiteness of the rotation matrix $\bar{e}^{\hat{\xi}_i \theta_i}$ is equivalent to $|\theta_i| < \frac{\pi}{2}$. This assumption is made in order to avoid a singular point, which is inevitable when the $SO(3)$ space is considered.

D. Communication Delays

In this subsection, we consider output synchronization in the presence of communication delays. In such a case, the output synchronization is redefined as

$$\lim_{t \rightarrow \infty} \psi(g_j(t - T_{ji})^{-1} g_i(t)) = 0, \forall i, j, j \neq i, \quad (18)$$

where $T_{ij} \geq 0$ is the summation of delays in the communication from the i -th rigid-body to the j -th rigid-body. Accordingly, we modify the input (3) as

$$V_i^b = K_i \sum_{j \in \mathcal{N}_i} w_{ij} \begin{bmatrix} e^{-\hat{\xi}_i \theta_i} & 0 \\ 0 & I \end{bmatrix} \begin{bmatrix} p_j(t - T_{ji}) - p_i(t) \\ \text{sk}(e^{-\hat{\xi}_i \theta_i(t)} e^{\hat{\xi}_j \theta_j(t - T_{ji})}) \end{bmatrix}. \quad (19)$$

Then, we have the following corollary.

Corollary 1: Suppose that there exist n rigid-bodies represented by (1). Then, under the assumption A1, the velocity input (19) achieves the output synchronization in the sense of (18) if $e^{\hat{\xi}_i \theta_i} \forall i$ are positive definite.

Proof: This corollary is proven in the same way as Theorem 1 by using the following potential function,

$$U_{\text{delay}} := \sum_{i=1}^n \gamma_i U_i(t) + \sum_{i=1}^n \sum_{j \in \mathcal{N}_i} \int_{t-T_{ji}}^t \gamma_i w_{ij} U_i(\tau) d\tau, \quad (20)$$

where $U_i := \frac{1}{2k_{pi}} \|p_i\|^2 + \frac{1}{k_{ei}} \phi(e^{\hat{\xi}_i \theta_i})$. ■

IV. NUMERICAL SIMULATIONS AND EXPERIMENTS

In this section, we numerically and experimentally demonstrate that the present input (3) achieves output synchronization.

A. Numerical Simulations

We first show numerical simulations with 5 rigid-bodies whose interaction is represented by the graph in Figure 3. The weighted graph Laplacian (2) and its left eigenvector corresponding to the eigenvalue equal to 0 are given by

$$L_w = \begin{bmatrix} 0.1 & -0.1 & 0 & 0 & 0 \\ -0.2 & 0.4 & -0.2 & 0 & 0 \\ 0 & 0 & 0.3 & -0.3 & 0 \\ 0 & 0 & 0 & 0.4 & -0.4 \\ -0.5 & 0 & 0 & 0 & 0.5 \end{bmatrix} \gamma = \begin{bmatrix} 0.9466 \\ 0.2367 \\ 0.1578 \\ 0.1183 \\ 0.0947 \end{bmatrix}. \quad (21)$$

Notice that all the elements of γ are positive. The desired linear and angular velocity are $v_d = [1 \ 0 \ 0]^T, \omega_d = [0 \ 0 \ 0]^T$, which means that all the rigid bodies finally move in the same direction as x axis of the world frame without rotating. The input (3) with $k_{pi} = 2$ and $k_{ei} = 2 \forall i$ is applied to each rigid-body under the following initial conditions.

$$\begin{aligned} p_1(0) & = [1 \ 0 \ 3]^T & \xi_1 \theta_1(0) & = [-0.21 \ -0.50 \ 0.77]^T \\ p_2(0) & = [2 \ -1 \ 2]^T & \xi_2 \theta_2(0) & = [0.60 \ 0.04 \ 0.83]^T \\ p_3(0) & = [3 \ 1 \ 2]^T & \xi_3 \theta_3(0) & = [-0.21 \ 0.77 \ -0.50]^T \\ p_4(0) & = [-1 \ -2 \ 0]^T & \xi_4 \theta_4(0) & = [-0.63 \ 0.37 \ -0.64]^T \\ p_5(0) & = [0 \ 0 \ 0]^T & \xi_5 \theta_5(0) & = [-0.77 \ 0.50 \ -0.21]^T \end{aligned}$$

Figure 4 shows the trajectory and attitude of each rigid-body and Figure 5 its position and rotation vector. In Figure 4, the

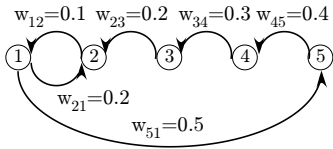


Fig. 3. Graph Topology in Simulation

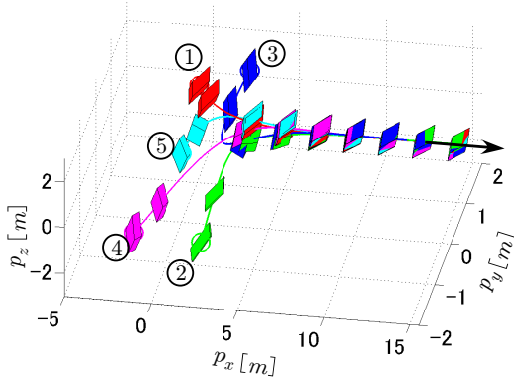


Fig. 4. Simulation Result

encircled number is associated with the corresponding one in Figure 3. In Figure 5 the rotation vectors $\xi_i \theta_i$ and positions p_i asymptotically converge to a common value at around 10 [s]. We also see from these figures that every rigid body moves in the prescribed direction after sufficiently long time has passed. Thus, each rigid finally moves with a desired velocity.

B. Experiments

In this section we present experimental results on a planar (2D) test bed. Figure 6 illustrates the experimental environment including the vehicles, camera, PC, and CF transmitters. The four vehicles (see Figs. 7) communicated by the graph in Figure 9 are controlled by a digital signal processor (DSP) from dSPACE Inc., which utilizes a power PC running at 2.8GHz. Control programs are written in MATLAB and SIMULINK, and implemented on the DSP using the Real-Time Workshop and dSPACE Software such as ControlDesk, RealTime Interface and so on. A MTV-7310 camera is mounted above the vehicles has a resolution of 470×570 . The video signals are available in real time via a frame grabber board PicPort-Stereo-HrD and image processing software HALCON. The sampling period of the controller and the frame rate provided by the camera are 0.33[ms] and 30 [fps], respectively. The position and orientation of the rigid-bodies are calculated by using the image processing.

In order to implement kinematic control on the vehicle network, we first designed a local PI controller *a priori* to track reference signals and then input the kinematic control laws as velocity reference signals (See Figure 8).

We input to each rigid-body the present input (3) with $k_{pi} = 0.1, k_{ei} = 0.1, w_{ij} = 1 \forall i, j$ and

- (A) $v_d = [0 \ 0]^T \quad \omega_d = 0,$
- (B) $v_d = [1.5 \ 0]^T \quad \omega_d = 0,$
- (C) $v_d = [1.5 \ \cos 1.5t]^T \quad \omega_d = 0.$

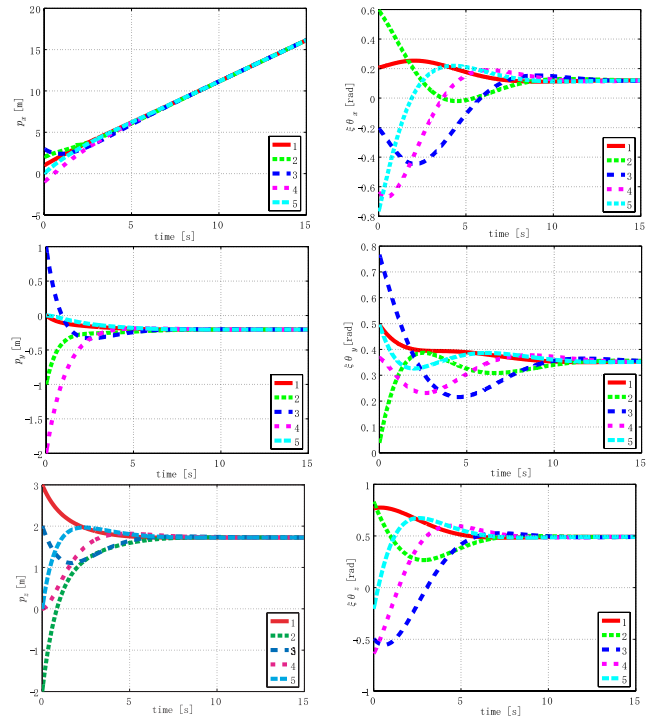


Fig. 5. Position p and Rotation Vector $\xi \theta$ in Simulation

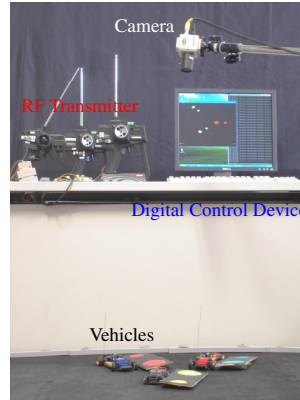


Fig. 6. Experiment Environment



Fig. 7. Vehicles

The desired velocity in case (A) means that we have no desired behavior. In this case each rigid body stops as some place after the output synchronizes. In case (B) all of rigid bodies move in the same direction as x axis in the world frame like the simulation case, and in case (C) move along a smooth sin curve after a period of time.

It should be noted that though all the rigid-bodies should be located on almost the same position after a sufficiently long time in order to achieve output synchronization, in experiments, this leads to the collision between rigid-bodies. We thus switch the input from (3) to the one in if the distances of all the vehicles becomes smaller than 20[cm].

Figs. 10, 11 and 12 illustrate the experimental results. These figures show that convergence of orientations is attained and the distances between vehicles decrease below 20[cm] at around 9[s]. Thus the output synchronization is almost achieved and every vehicle converges to a desired

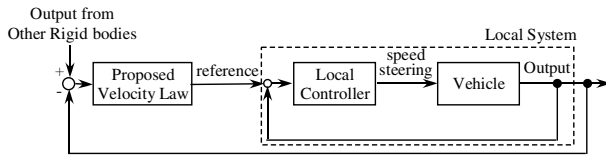


Fig. 8. Local Control System



Fig. 9. Graph Topology in Experiment

velocity v_d after a reasonable amount of time.

Strictly speaking, the vehicles have nonholonomic constraints. Although these are not still considered theoretically, we believe that the result of this paper can be extend to rigid-bodies with nonholonomic constraints via similar techniques in [22].

V. CONCLUSIONS

In this paper, we have considered the output synchronization problem on strongly connected graphs. A velocity control law has been developed based on the passivity property to achieve the output synchronization. The convergence is proven from the fact that strongly connected graphs have a left eigenvector of the weighted graph Laplacian associated with eigenvalue 0 whose all elements are positive. Moreover we have shown the facts that the present input still attains output synchronization in the case with communication delay. The simulation and experimental results have demonstrated the validity of our results.

Future researches will be directed to the introduction of visual sensors [11]. We will also tackle the output synchronization problem including the dynamics of each rigid-body by using passivity-based control.

Acknowledgement : The author would like to thank Mr. N. Kobayashi for invaluable help in carrying our the experiments.

REFERENCES

- [1] V. Kumar, N. Leonard, A. S. Morse, eds., *Cooperative Control : A Post-workshop Volume 2003 Block Island Workshop On Cooperative Control, Lecture Notes in Control and Information Sciences*, vol. 309, Springer, 2004.
- [2] R. O. Saber, J. A. Fax and R. M. Murray, "Consensus and Cooperation in Networked Multi-Agent Systems," *Proc. of the IEEE*, vol. 95, no. 1, 2007.
- [3] A. Jadbabaie, J. Lin and A. S. Morse, "Coordination of groups of mobile autonomous agents using nearest neighbor rules," *IEEE Trans. on Automatic Control*, vol. 48, no. 6, pp. 988–1001, 2003.
- [4] H. Tanner, A. Jadbabaie, and G. J. Pappas, "Flocking in Fixed and Switching Networks," *IEEE Trans. on Automatic Control*, vol. 52, no. 5, pp. 863–868, 2007.
- [5] R. O. Saber, "Flocking for Multi-Agent Dynamic Systems: Algorithms and Theory," *IEEE Trans. on Automatic Control*, vol. 51, no. 3, pp. 401–420, 2006.
- [6] D. J. Lee and M. W. Spong, "Stable Flocking of Multiple Inertial Agents on Balanced Graphs," *IEEE Trans. on Automatic Control*, vol. 52, no. 8, pp. 1469–1475, 2007.
- [7] N. Chopra and M. W. Spong, "Output Synchronization of Nonlinear Systems with Time Delay in Communication," *Proc. of the 45th IEEE Conference on Decision and Control*, pp. 4986–4992, 2006.
- [8] N. Chopra and M. W. Spong, "Passivity-Based Control of Multi-Agent Systems," in *Advances in Robot Control: From Everyday Physics to Human-Like Movements*, S. Kawamura and M. Svinin, eds., pp. 107–134, Springer, 2006.

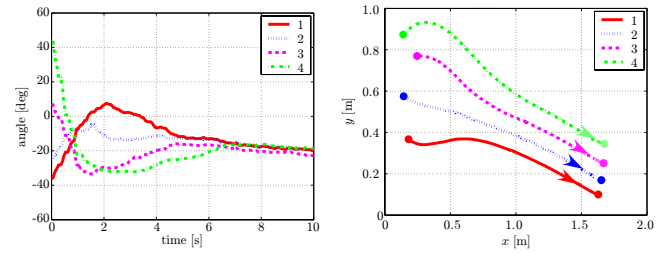


Fig. 10. Experiment Result 1 ($v_d = [0 \ 0]^T$)

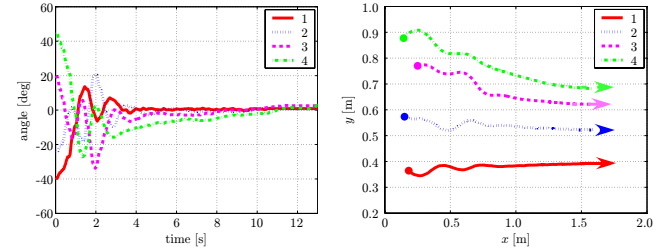


Fig. 11. Experiment Result 2 ($v_d = [1.5 \ 0]^T$)

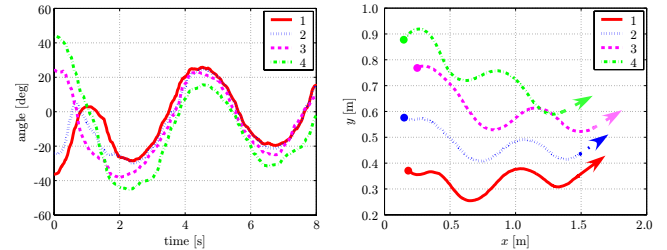


Fig. 12. Experiment Result 3 ($v_d = [1.5 \ \cos 1.5t]^T$)

- [9] I.-A. F. Ihle, M. Arcak and T. I. Fossen, "Passivity-Based Designs for Synchronized Path Following," *Automatica*, vol. 43, no. 9, pp. 1508–1518, 2007.
- [10] Y. Igarashi, T. Hatanaka, M. Fujita and M. W. Spong, "Passivity-based 3D Attitude Coordination: Convergence and Connectivity," *Proc. of the 46th IEEE Conference on Decision and Control*, pp. 2558–2565, 2007.
- [11] M. Fujita, H. Kawai and M. W. Spong, "Passivity-based Dynamic Visual Feedback Control for Three Dimensional Target Tracking: Stability and L2-gain Performance Analysis," *IEEE Trans. on Control Systems Technology*, vol. 15, no. 1, pp. 40–52, 2007.
- [12] L. Scardovi, R. Sepulchre and N. E. Leonard, "Stabilization Laws for Collective Motion in Three Dimensions," *Proc. of the 2007 European Control Conference*, pp. 4591–4597, 2007.
- [13] A. Sarlette, R. Sepulchre and N. E. Leonard, "Autonomous rigid body attitude synchronization," *Proc. of the 46th IEEE Conference on Decision and Control*, pp. 2566–2571, 2007.
- [14] R. Murray, Z. Li and S. S. Sastry, *A Mathematical Introduction to Robotic Manipulation*, CRC Press, 1994.
- [15] F. Bullo and A. D. Lewis, *Geometric Control of Mechanical Systems*, Springer, 2004.
- [16] M. W. Spong, S. Hutchinson and M. Vidyasagar *Robot Modeling and Control*, John Wiley & Sons, Inc., New York, 2006.
- [17] Wei Ren, "Multi-vehicle consensus with a time-varying reference state," *Systems & Control Letters*, vol. 56, pp. 474–483, 2007.
- [18] N. Moshtagh and A. Jadbabaie, "Distributed Geodesic Control Laws for Flocking of Nonholonomic Agents," *IEEE Trans. on Automatic Control*, vol. 52, no. 4, pp. 681–686, 2007.
- [19] W. Ren and E. Atkins, "Distributed multi-vehicle coordinated control via local information exchange," *International Journal of Robust and Nonlinear Control*, Vol. 17, No. 10–11, pp. 1002–1033, 2007.
- [20] H. K. Khalil, *Nonlinear Systems, Third Edition*, Prentice Hall, 2002.
- [21] R. A. Horn and C. R. Johnson, *Matrix analysis*, Cambridge University Press, 1985.
- [22] D. V. Dimarogonas and K. J. Kyriakopoulos, "On the Rendezvous Problem for Multiple Nonholonomic Agents," *IEEE Trans. on Automatic Control*, vol. 52, no. 5, pp. 916–922, 2007.